Effect of Fe and Co substitution on the martensitic stability and the elastic, electronic, and magnetic properties of Mn_2NiGa: Insights from *ab initio* calculations

Ashis Kundu,* Sheuly Ghosh, and Subhradip Ghosh†
Department of Physics, Indian Institute of Technology Guwahati, Guwahati 781039, Assam, India
(Received 8 August 2017; published 10 November 2017)

We investigate the effects of Fe and Co substitutions on the phase stability of the martensitic phase and mechanical, electronic, and magnetic properties of the magnetic shape memory system Mn_2NiGa by first-principles density functional theory calculations. The evolution of these aspects upon substitution of Fe and Co at different crystallographic sites is investigated by computing the electronic structure, mechanical properties (tetragonal shear constant, Pugh ratio, and Cauchy pressure), and magnetic exchange parameters. We find that the austenite phase of Mn_2NiGa gradually stabilizes with increase in concentration of Fe/Co due to the weakening of the minority spin hybridization of Ni and Mn atoms occupying crystallographically equivalent sites. The interplay between relative structural stability and the compositional changes is understood from the variations in the elastic moduli and electronic structures. We find that like in the Ni_2MnGa-based systems, the elastic shear modulus C' can be considered as a predictor of composition dependence of martensitic transformation temperature T_m in substituted Mn_2NiGa, thus singling it out as the universally acceptable predictor for martensitic transformation in Ni-Mn-Ga compounds over a wide composition range. The magnetic properties of Mn_2NiGa are found to be greatly improved by the substitutions due to stronger ferromagnetic interactions in the compounds. The gradually weaker (stronger) Jahn-Teller distortion (covalent bonding) in the minority spin densities of states due to substitutions leads to a half-metallic-like gap in these compounds resulting in materials with high spin polarization when the substitutions are complete. The substitutions at the Ga site result in the two compounds Mn_2NiFe and Mn_2NiCo with very high magnetic moments and Curie temperatures. Thus, our work indicates that although the substitutions destroy the martensitic transformation and thus the possibility of realization of shape memory properties in Mn_2NiGa, magnetic materials with very good magnetic parameters that are potentially useful for novel magnetic applications can be obtained. This can trigger interest in the experimental community in further research on substituted Mn_2NiGa.

DOI: 10.1103/PhysRevB.96.174107

I. INTRODUCTION

Magnetic shape memory alloys (MSMAs) have drawn much attention in recent years due to their multiple functional properties such as magnetic field induced strain (MFIS), large magnetocaloric effect, and magnetoresistance [1–10]. The MFIS is useful for magnetomechanical actuators [1,3], and large magnetocaloric effect is associated with magnetostructural coupling [11], useful for magnetic refrigeration.

Among many MSMAs, the Heusler Ni-Mn-Ga system has been explored extensively. The reason is that several modulated martensite phases were observed in this system with the composition ratio of Ni, Mn, and Ga near 2:1:1, which is close to that of Ni_2MnGa. These modulated phases were intermediate phases during the martensitic transformation from the high-temperature Heusler phase to a nonmodulated tetragonal phase and had yielded MFIS as large as 6% and 10% [2,3,12,13]. However, a martensitic transformation temperature (T_m) of about 200 K and a Curie temperature (T_c) of about 380 K [14] were serious hindrances in exploiting the multifunctionalities of Ni_2MnGa. This is because of the following facts: First, T_m being lower than room temperature makes the commercial realization of the material for shape memory applications difficult, and second, the large difference in T_m and T_c makes it impossible to get the maximum of the magnetocaloric effect as it requires the transition point for martensitic and magnetic transitions very close [15].

Controlled substitution of one element with another is a standard procedure for achieving target properties of materials. In order to optimize the thermodynamic parameters without compromising much on the other important properties for functional applications such as MFIS, substitution of each one of the constituents in Ni_2MnGa with other transition metals Fe, Co, and Cu have been attempted. The outcomes of these attempts are mixed and provide useful insights into the fundamental physics of this system which can be useful in designing this material with target properties. A larger MFIS of about 12% was observed in the nonmodulated tetragonal phase of Ni_2MnGa upon substitution of all three elements by 4% of Co and Cu each [16]. Several investigations with substitution of a single type of transition metal into different sublattices have also been carried out. The outcome of substitution at the Ni site is substantial reduction of T_m with slight improvement in T_c [17–19], irrespective of whether the substituting element is Fe, Co, or Cu. Substitution at the Mn site, on the other hand, produced results depending on the substituting element. While substitution of Mn by Co or Cu elevates T_m and reduces T_c as the concentration of the substituting element increases [20–22], T_m is observed to decrease as a function of Fe concentration when Fe is substituted at the Mn site. Substitution at the Ga site by either Fe, Co, or Cu shows a trend of rapid increase in T_m and slow decrease of T_c, resulting in them coinciding for the concentration of the substituting element in the range of 10%–20% [22–24]. These outcomes,

*k.ashis@iitg.ernet.in
†subhra@iitg.ernet.in

thus, prove that the structure-property relationships in Ni-Mn-Ga-based systems delicately depend on the substituting element, the substituent, and the composition.

Mn_2NiGa is a MSMA with thermodynamic parameters T_m and T_c much better than those of Ni_2MnGa, from the point of view of applications. It shows a martensitic transformation from the high-temperature Hg_2CuTi (inverse Heusler) phase to a nonmodulated (NM) tetragonal phase with T_m equal to 270 K [25,26], very close to room temperature. The Curie temperature, T_c, of this material is 588 K [25,26], much higher than that of Ni_2MnGa, which guarantees a magnetically ordered phase well above room temperature. Both are desirable for the actuator applications at room temperature. Experimentally a MFIS of 4% was observed in the NM tetragonal structure which was still unsaturated in a magnetic field of 1.8T [25], implying that a larger MFIS can be obtained with larger field. In recent density functional theory (DFT) based investigations, a number of modulated phases were predicted [27], some of which were observed in experiments [28,29] as well. The DFT calculations predicted that larger MFIS can be realized in the modulated phases. Very recently, a large inverse magnetocaloric effect has also been reported in this system [30]. Therefore, Mn_2NiGa meets the requirements of a MSMA with multiple functionalities, often better than the prototype Ni_2MnGa.

In spite of having reasonable and more desirable functional properties, one crucial issue with Mn_2NiGa is its low value of magnetization which is about 1.2 μ_B per formula unit as opposed to more than 4 μ_B per formula unit in Ni_2MnGa. This happens due to a ferrimagnetic ground state arising out of antiparallel orientation of the two Mn atoms. Substitution by another magnetic atom such as Co, Fe, and Cu could be a useful way to adjust the magnetic interactions in the parent alloys, thus improving the magnetization primarily. With this motivation, Luo *et al.* substituted Mn with Fe in Mn_2NiGa [31]. They observed an increase in the saturation magnetization with increasing Fe concentration. However, both T_m and T_c decrease with increasing Fe content and no martensitic transformation is observed beyond 30% of the Fe content [31]. Ma *et al.* investigated the effect of Co substitution at Ni and Ga sites of Mn_2NiGa through magnetization measurement and *ab initio* calculations [32]. They found a remarkable threefold jump in the saturation magnetization when Co is substituted at Ga sites which, by means of *ab initio* calculation, was attributed to a complex sublattice occupancy pattern. Though Co substitution at the Ni site was not as dramatic, the magnetization improved which was explained by means of increasing ferromagnetic component in a ferrimagnetic host. In both cases, the martensitic transformation vanished rapidly indicating stabilization of the the inverse Heusler phase down to low temperature. A different variation of T_c with Co content was observed depending on the site of substitution. Very recently, DFT calculations on Cu-doped Mn_2NiGa reported that T_m decreases when Cu is substituted at Mn and Ni sites but increases when substituted at the Ga site [33].

The investigations on substitution of another transition metal in Mn_2NiGa are thus quite scattered. However, they offer very interesting perspectives, both for fundamental understanding as well as for engineering materials with target properties. The number of valence electron per atom (e/a) was identified to be a predictor of T_m with $T_m \sim$ e/a [34–36] for systems undergoing martensitic transformations. In the case of off-stoichiometric Ni_2MnGa alloys and Fe, Co, and Cu substituted Ni_2MnGa alloys e/a was found not to correlate with T_m [37–40]. Instead, the shear modulus C' was found to be a better predictor for composition dependence of T_m [38,39]. On the other hand, ΔE, the energy difference between the high-temperature Heusler phase and the low-temperature NM tetragonal phase, was found to correlate well with C' and T_m for a number of systems in the Ni-Mn-Ga family [41,42]. Experimental results on substituted Mn_2NiGa [31,32] indicate that e/a does not correlate with T_m. On the other hand, the variations of T_c and magnetization in substituted Mn_2NiGa depend, both quantitatively as well as qualitatively, not only on the nature of the element that is being substituted. Another noteworthy point is the gradual stabilization of the high-symmetry inverse Heusler phase with substitution, irrespective of the chemical identity of the substituting atom and the site on which it is being substituted, in substituted Mn_2NiGa. Recent DFT calculations of magnetic moments and the electronic structures in two compounds, MnCoNiGa and MnFeNiGa, predict that the compounds are nearly half metals [43]. We note that these two compounds can be obtained by substituting 50% of the total Mn content in Mn_2NiGa. This implies that the substitution of Mn in Mn_2NiGa would potentially give rise to materials with different functional properties. Given these findings, one needs a systematic first-principles-based investigation addressing the multiple issues under a single approximation, in order to provide a fundamental understanding of the interrelations between composition, sublattice occupancy, phase stability, and magnetic interactions. An investigation along this line would help to tune the necessary parameters for targeted applications in Mn_2NiGa-based systems and possibly in Ni-Mn-Ga systems over a wide composition range.

In this paper, we report the outcome of substitution of 25%, 50%, 75%, and 100% Fe and Co at different sites of the parent compound Mn_2NiGa. Specifically, we have looked at the patterns of site occupancies upon a particular substitution, the stabilities of the martensitic NM phases, the elastic properties, the total and atomic magnetic moments, the effective magnetic exchange interactions, and the magnetic transition temperatures and their variations upon substitution at different sites. The results are interpreted from the composition dependencies of the computed electronic structures. This approach enables us to pinpoint the microscopic origin of the martensitic phase stability upon different substitutions, the variations in the magnetic properties with compositions and nature of the substitutions, and the variations in the mechanical properties and their interrelations with the nature of the martensitic stability, and most importantly to establish a predictor for variations in T_m. Another outcome of this investigation is the prediction of a material with high magnetization and high T_c which can be used in various applications which require large moment and stability of the magnetically ordered phase and which can fall in the same class of X_2YZ materials with Heusler or Heusler-like structures where all three components have unfilled d shells [44].

The paper is arranged as follows: In Sec. II, the first-principles computational method and the calculational details are provided. In Sec. III, the results of our calculations and

their analysis are presented. The final remarks on this work are presented in Sec. IV.

II. COMPUTATIONAL METHODS

The total energies, the electronic structures, and the magnetic moments were calculated with the spin-polarized density functional theory (DFT) based projector augmented wave (PAW) method as implemented in the Vienna *Ab initio* Simulation Package (VASP) [45–47]. For all calculations, we have used the Perdew-Burke-Ernzerhof implementation of the generalized gradient approximation (GGA) for the exchange-correlation functional [48]. An energy cutoff of 450 eV and a Monkhorst-Pack [49] $11 \times 11 \times 11\,k$ mesh were used for self-consistent calculations. A larger k mesh of $15 \times 15 \times 15$ was used for the calculations of the electronic structures. The convergence criteria for the total energies and the forces on individual atoms were set to 10^{-6} eV and 10^{-2} eV/Å, respectively. To investigate the stability of the substituted compounds, we have calculated the formation energy for each system, which can be obtained in the following way,

$$E_f = E_{\text{tot}} - \sum_i n_i E_i. \tag{1}$$

E_{tot} is the ground state total energy of a system, E_i is the ground state energy of the ith component in its elemental phase, and n_i is its concentration in the system under consideration. The elastic constants for the compounds are calculated using the energy-strain method [50–52] only for their high-temperature phases with cubic symmetry. The details of the calculations are given in [53].

The magnetic pair exchange parameters are computed in order to understand the nature of the magnetic interactions in these systems. They are efficiently calculated using the multiple-scattering Green's function formalism as implemented in the SPRKKR code [54]. In this approach, the spin part of the Hamiltonian is mapped to a Heisenberg model:

$$H = -\sum_{\mu,\nu}\sum_{i,j} J_{ij}^{\mu\nu}\mathbf{e}_i^{\mu}\cdot\mathbf{e}_j^{\nu}. \tag{2}$$

μ, ν represent different sublattices; i, j represent atomic positions; and $\mathbf{e}_i^{\mu}$ denotes the unit vector along the direction of magnetic moments at site i belonging to sublattice μ. The $J_{ij}^{\mu\nu}$ are calculated from the energy differences due to infinitesimally small orientations of a pair of spins within the formulation of Liechtenstein *et al.* [55]. In order to calculate the energy differences by the SPRKKR code, a full-potential spin-polarized scaler relativistic Hamiltonian with angular momentum cutoff $l_{\max} = 3$ is used along with a converged k mesh for Brillouin zone integrations. The Green's functions are calculated for 32 complex energy points distributed on a semicircular contour. The energy convergence criterion was set to 10^{-5} eV for the self-consistency cycles. The equilibrium lattice parameters obtained from the PAW calculations were used in these calculations. These exchange parameters are then used for the calculations of Curie temperatures (T_c). The Curie temperatures are estimated with two different approaches: the mean-field approximation (MFA) [56] and the Monte Carlo simulation (MCS) method [57] in order to check the qualitative consistency in the results and to obtain a reliable estimate of the quantity as the MFA is known to overestimate T_c while the MCS method is more accurate quantitatively. Details of the MFA and MCS calculations are given in [53].

III. RESULTS AND DISCUSSION

At high temperature, Mn_2NiGa crystallizes in the Hg_2CuTi (inverse Heusler) structure (space group No. 216; $F\bar{4}3m$) with four inequivalent Wyckoff positions (4a, 4b, 4c, 4d) in an fcc unit cell [25,58]. The Mn atoms occupy the 4a (0, 0, 0) and 4c (0.25, 0.25, 0.25) Wyckoff positions; we denote them as MnI and MnII, respectively. The 4b (0.5, 0.5, 0.5) and 4d (0.75, 0.75, 0.75) positions are occupied by Ni and Ga, respectively. In this work, we focus on the high-temperature phase as results obtained in this phase would be enough for most of the physical understanding about the effects of substituting another magnetic element on the functional properties of Mn_2NiGa. To model the chemical substitution, we have taken a 16-atom conventional cubic cell. Thus, chemical substitution of 25%, 50%, 75%, and 100% can be modeled by successive replacement of the atoms of one of the constituents. For example, to make a 25% Co substitution at the Ni site, one Ni atom out of the four in the 16 atom cell is to be replaced with one Co atom. This modeling strategy has worked well in cases of investigations on chemically substituted Ni_2MnGa [59,60].

A. Site preferences, stability, and structural parameters

The site occupancies in a substituted system have an important impact on the physical properties of the system. Thus, before proceeding with computations of the physical properties, the site preferences of the substituting atom are to be decided. If the substituting atom occupies the site of the substituted element, the configuration is "normal"; otherwise it is termed "abnormal". The preferred site occupancy is determined by comparing the total energies of the two configurations. In the case of Fe and Co substituted Ni_2MnGa, free-energy calculations revealed that the preferred configuration in cases of substitutions at Ni or Mn sites are "normal" whereas the substitution at Ga site prefers an "abnormal" configuration [substituting Fe (Co) occupies the Mn (Ni) sites while the rest of the Mn (Ni) move to Ga sites] [39]. For Cu-substituted Ni_2MnGa, the preferred configuration always is the "normal" one [39]. In the case of Co and Cu substituted Mn_2NiGa, the trend of site occupancy is found to be quite similar to that of substituted Ni_2MnGa systems [32,33]. It has been observed that in Heusler alloys, the following pattern of site occupancy is generally followed: the substituting transition-metal atom will prefer the 4a and 4b sites if it has a larger number of valence electrons, while it will prefer the 4c and 4d sites if the number of valence electrons is less [61–65]. This has been observed even in cases of antisite disorder in Mn_2NiZ alloys [66,67]. So the substituting Fe or Co in Mn_2NiGa would prefer the MnI sites over MnII sites if Mn atoms were being substituted, as Fe and Co both have larger numbers of valence electrons than Mn. We have verified this by comparing the total energies of two cases: one, where the entire Fe/Co occupies MnI sites and two, Fe/Co are equally distributed among the two Mn

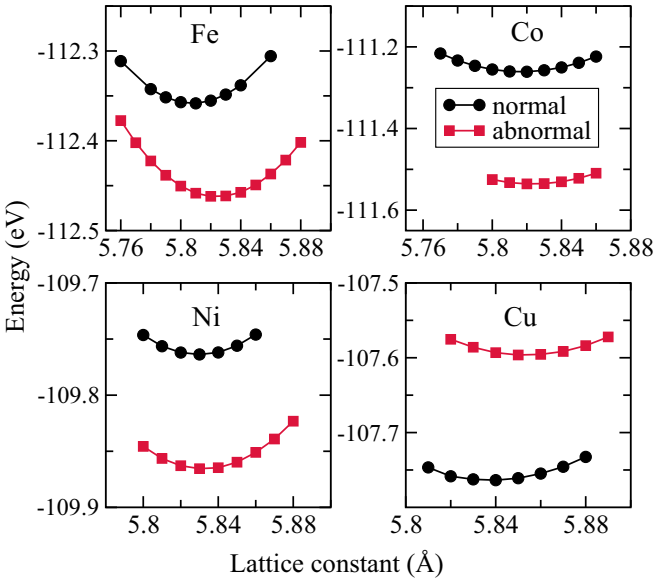

FIG. 1. Calculated total energy as a function of lattice constant for 25% Fe, Co, Ni, and Cu substituted at the Ga site in $Mn_2NiGa(Mn_2NiGa_{0.75}X_{0.25})$. "normal": Fe, Co, Ni, or Cu occupy the Ga sublattice; "abnormal": Fe, Co, Ni, or Cu occupy the MnI sites and remaining MnI atoms move to Ga sites.

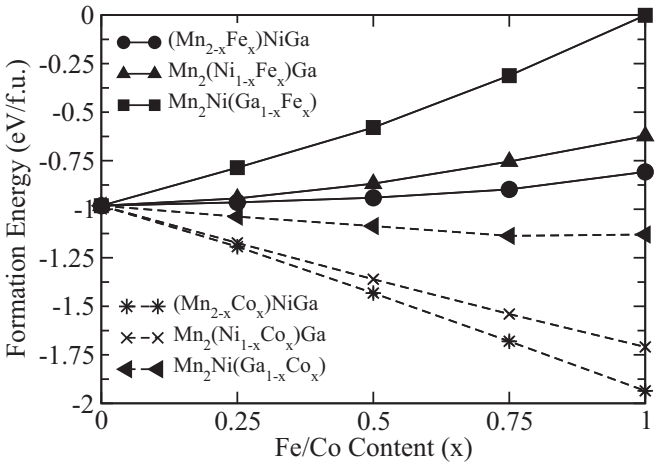

FIG. 2. Formation energy (eV/f.u.) as a function of Fe and Co content substituted at different sites in Mn_2NiGa.

sites. For substitution of Fe or Co at the Ni site, we find the "normal" site occupancy (Fe/Co occupying Ni sites) to be energetically favorable. This is consistent with the general pattern described above and the previous first-principles results on Co-substituted Mn_2NiGa [32]. The substitution at the Ga site, however, follows a different pattern, depending on the substituting element. In the case of Co substitution at the Ga site in Mn_2NiGa, earlier work [32] showed that the Co prefers to occupy the MnI sites pushing the remaining MnI atoms to Ga sites (henceforth denoted as MnIII). This can be understood on the basis of the general occupancy pattern in Heusler alloys described above: since Co has more valence electrons than Mn and Ga, it will occupy the MnI sites and the remaining MnI will occupy the Ga sites and would be distinguished from MnI and MnII by being denoted as MnIII. In order to check whether this is indeed the case with both Fe- and Co-substituted system, we have computed the total energies for "normal" and "abnormal" configurations. The results for 25% substitution are shown in Fig. 1. For comparison, we have also shown the results for Ni and Cu substitution at Ga sites. The results suggest that the "abnormal" site occupancies are preferable for Fe, Co, and Ni substitutions at Ga sites of Mn_2NiGa while Cu substitution prefers a "normal" configuration. This exactly follows the trend obtained in substituted Ni_2MnGa [39]. We can thus conclude that the site preferences of the substituting transition-metal atom in Ni-Mn-Ga systems is dependent on the valence shell electronic configurations of both the atom that is being substituted and the substituting atom.

After fixing the site preferences of the atoms in substituted Mn_2NiGa, we computed the equilibrium lattice constants and the formation energies of the compounds obtained by chemical substitutions at various sites in the cubic Hg_2CuTi phase. The results are presented in Table I. For all the cases, the equilibrium lattice constants decrease linearly with increasing concentration of the substituting element. For most of the cases, this trend can be explained from the variations of atomic radii of the host (the atomic radii of Mn, Ni, and Ga are 1.27 Å, 1.24 Å, and 1.35 Å, respectively) and the substituting elements (the atomic radii of Fe and Co are 1.26 Å and 1.25 Å, respectively). The only exceptions are the substitutions at the Ni site where instead of an expected increase in the lattice constant with concentration of the substituting element, the lattice constant decreases. Thus, the trends in the variations in the lattice constants cannot be understood in terms of differences in atomic radii alone, and other effects such as bonding and magnetism are expected to play roles as was noted earlier [33,39]. Another noteworthy point is that while the trends in the variations of the lattice constants obtained in this calculations qualitatively agree with those observed in the experiments on Fe substituted at Mn sites [31] and Co substituted at Ga sites of Mn_2NiGa [32], the experimentally observed trends are opposite to our calculated results in cases of Co substituted at the Ni sites [32]. Experimentally, it is found that the lattice constant increases with increasing concentration of Co when it is substituted at the Ni site, although the increase is very slow (about 0.1% maximum). Thus, the calculated trends are consistent with the experiments for most of the systems under consideration here.

In Fig. 2, we present the variations in formation energies of compounds with Fe or Co substituted at different sites in Mn_2NiGa as a function of the concentration of the substituent. We have considered bcc-Fe, hcp-Co, fcc-Ni, orthorhombic Ga, and antiferromagnetic bcc-Mn as ground state structures in their elemental phases. It can be seen that the formation energy is negative for all systems except Mn_2NiFe ($E_f = 0$). This implies that except for Mn_2NiFe all the compounds can form in the Hg_2CuTi structure from an enthalpy point of view. We have not come across any experimental result regarding Mn_2NiFe contradicting this finding. As some of the compounds under investigation such as $Mn_{2-x}Fe_xNiGa$ ($x = 0$–0.5) [31], $Mn_2Ni_{1-x}Co_xGa$ ($x = 0$–0.5), and $Mn_2NiGa_{1-x}Co_x$ ($x = 0$–0.52) [32] have already been synthesized, our DFT calculations correctly reproduce the experimental observations

TABLE I. Calculated values of equilibrium lattice constants (a_0), electron to atom ratios (e/a), and the formation energies (E_f) of various compounds in the Hg_2CuTi phase are given. The total energy differences (ΔE) between the austenite (Hg_2CuTi) phase and the martensite (tetragonal) phase [the equilibrium value of (c/a), the tetragonal distortion, is given in parentheses] and the corresponding volume changes ($|\Delta V|/V$) with respect to the equilibrium volume in the Hg_2CuTi phase are given in the 5th and 6th columns. M_A is the total magnetic moment in μ_B/f.u. of the austenite phase. Reported values of lattice constants and magnetic moments in the literature are also given.

System	a_0 (Å)	e/a	E_f (eV/f.u.)	ΔE (c/a) (mev/atom)	$\lvert\Delta V\rvert/V$ (%)	M_A (μ_B/f.u.)	a_0^{Lit} (Å)	M_A^{Lit} (μ_B/f.u.)
Mn_2NiGa	5.84	6.75	−0.98	26.98 (1.28)	0.65	1.16	5.91 [25,31], 5.85 [68,69], 5.88 [32]	1.14 [68], 1.18 [32]
$(Mn_{0.75}Fe_{0.25})NiMnGa$	5.83	6.8125	−0.96	8.55 (1.26)	0.98	1.72	5.88 [31]	1.55 [31]
$(Mn_{0.5}Fe_{0.5})NiMnGa$	5.81	6.875	−0.94			2.62	5.86 [31]	2.68 [31]
$(Mn_{0.25}Fe_{0.75})NiMnGa$	5.78	6.9375	−0.90			3.46		
FeNiMnGa	5.75	7	−0.81			4.02	5.799 [43]	4.01 [43], 3.45 [43]
Mn_2NiGa	5.84	6.75	−0.98	26.98 (1.28)	1.04	1.16		
$Mn_2(Ni_{0.75}Fe_{0.25})Ga$	5.82	6.625	−0.94	11.80 (1.30)	0.42	1.45		
$Mn_2(Ni_{0.5}Fe_{0.5})Ga$	5.80	6.5	−0.87	5.07 (1.34)	1.67	1.49		
$Mn_2(Ni_{0.25}Fe_{0.75})Ga$	5.79	6.375	−0.75	15.04 (1.38)	1.71	1.31		
Mn_2FeGa	5.78	6.25	−0.62	33.07 (1.40)	2.53	1.04	5.80 [70], 5.76 [69]	1.03 [69]
Mn_2NiGa	5.84	6.75	−0.98	26.98 (1.28)	0.65	1.16		
$Mn_2Ni(Ga_{0.75}Fe_{0.25})$	5.82	7.0625	−0.78	9.56 (1.30)	1.82	2.79		
$Mn_2Ni(Ga_{0.5}Fe_{0.5})$	5.80	7.375	−0.58			4.63		
$Mn_2Ni(Ga_{0.25}Fe_{0.75})$	5.77	7.6875	−0.31			6.40		
Mn_2NiFe	5.74	8	0.00			8.03		
Mn_2NiGa	5.84	6.75	−0.98	26.98 (1.28)	0.65	1.16		
$(Mn_{0.75}Co_{0.25})NiMnGa$	5.83	6.875	−1.19	18.57 (1.26)	0.43	1.97		
$(Mn_{0.5}Co_{0.25})NiMnGa$	5.81	7	−1.43			2.95		
$(Mn_{0.25}Co_{0.75})NiMnGa$	5.80	7.125	−1.68			3.78		
CoNiMnGa	5.78	7.25	−1.94			4.98	5.803 [43]	5.07 [43], 4.47 [43], 4.5 [18]
Mn_2NiGa	5.84	6.75	−0.98	26.98 (1.28)	0.65	1.16		
$Mn_2(Ni_{0.75}Co_{0.25})Ga$	5.82	6.6875	−1.17	18.51 (1.28)	0.02	1.46		1.52 [32]
$Mn_2(Ni_{0.5}Co_{0.5})Ga$	5.80	6.625	−1.36	7.00 (1.28)	1.02	1.71	5.88 [32]	1.70 [32]
$Mn_2(Ni_{0.25}Co_{0.75})Ga$	5.78	6.5625	−1.54			1.92		
Mn_2CoGa	5.76	6.5	−1.70			2.00	5.78 [69]	2.00 [69]
Mn_2NiGa	5.84	6.75	−0.98	26.98 (1.28)	0.65	1.16		
$Mn_2Ni(Ga_{0.75}Co_{0.25})$	5.82	7.125	−1.04	16.99 (1.30)	1.82	2.88		3.11 [32]
$Mn_2Ni(Ga_{0.5}Co_{0.5})$	5.81	7.5	−1.09			4.73	5.84 [32]	5.29 [32]
$Mn_2Ni(Ga_{0.25}Co_{0.75})$	5.80	7.875	−1.14			6.94		
Mn_2NiCo	5.79	8.25	−1.13			9.04		

and hence can provide guidance regarding the possibility of synthesizing the ones which have not been synthesized yet. Regarding the relative stabilities of compounds upon substitution of different atoms, our calculations imply that the substitution at different sites by Co is more favorable than substitution by Fe. Also the substitutions at the Ga sites make the compounds the least stable. By comparing the formation energies calculated here and in Ref. [33], we conclude that the Co substitution in Mn_2NiGa produces more stable compounds compared to the ones formed by substituting Fe or Cu. The origin of this lies in the differences in the electronic structures. We address this in Sec. III D.

B. Martensitic phase transformation

From the point of view of functionality, it is important to investigate the sustainability of the martensitic transition of Mn_2NiGa upon substitutions by various atoms. Experiments on Co substitution at Ni and Ga sites [32] did not find any martensitic transformation beyond 16% of Co in the system. The measurements on $Mn_2Co_{0.08}Ni_{0.92}Ga$ and $Mn_2Co_{0.08}NiGa_{0.92}$ showed that T_m decreases rapidly to 125 K and 103 K, respectively, from 270 K in the case of Mn_2NiGa. Fe substitution at the Mn site also led to a rapid decrease of T_m (120 K for $Mn_{1.7}Fe_{0.3}NiGa$) with no trace of martensitic transformation being observed beyond 30% of Fe. In this subsection, we examine the stabilities of the martensitic phases for all the compounds in order to find whether there is any trend with quantities such as (e/a) so that a predictor of variation in the T_m can be fixed. We do this by computing the total energy differences, ΔE, between the high-temperature Hg_2CuTi phases and the low-temperature nonmodulated martensitic phases with tetragonal structure, the later being obtained by tetragonal distortion of the former.

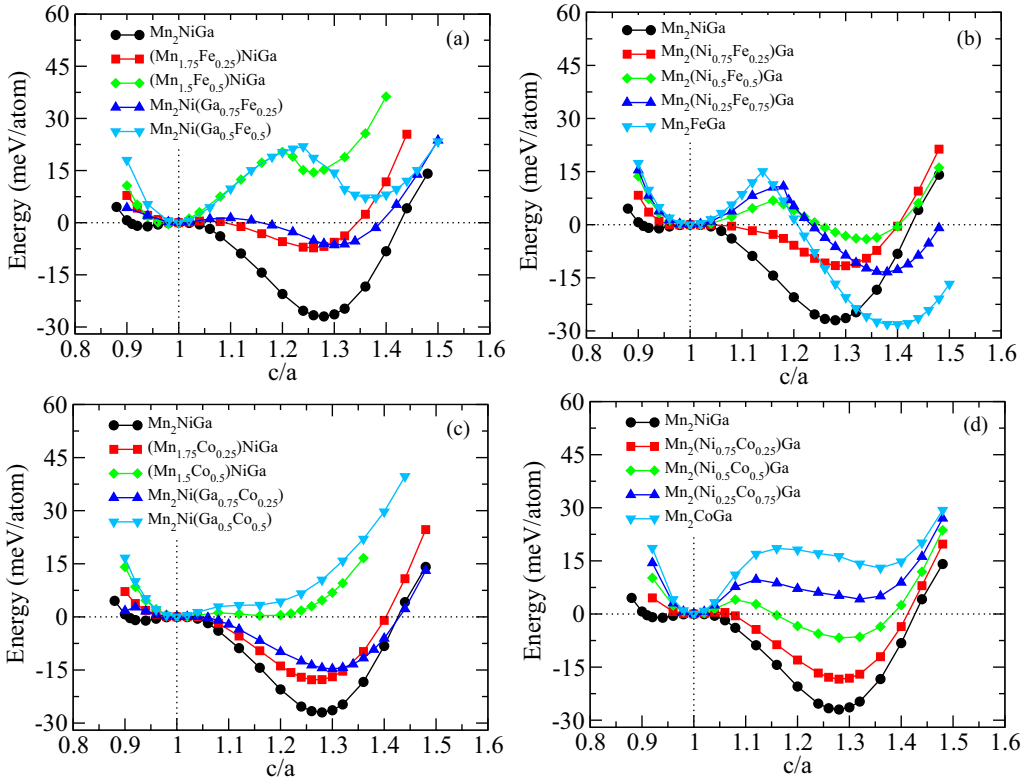

FIG. 3. The variations of total energies as a function of c/a ratio for Fe and Co substituted Mn_2NiGa compounds. The zero energy is taken to be the energy of the austenite phase.

While ΔE does not provide an accurate quantitative estimate of T_m as that requires inclusion of various contributions to the free energy which are difficult to compute for a chemically disordered system, its variations with compositions help make a heuristic predictions on qualitative variations of T_m and the stability of the martensitic phases. Such an approach has been adopted elsewhere [33,41] successfully.

In Fig. 3, we show the results of variations in the total energies with tetragonality (c/a) by keeping the volume constant at the equilibrium volume of Hg_2CuTi phases for each one of the Fe and Co substituted Mn_2NiGa systems. The reference energy in all cases is fixed at the one corresponding to $c/a = 1$, the Hg_2CuTi phase. From Figs. 3(a) and 3(c), it can be seen that the Fe or Co substitutions at Mn or Ga sites reduce the stabilities of the martensite phases as the values of ΔE decrease (see Table I) compared to the host Mn_2NiGa ($\Delta E = 26.98$ meV/atom) as the concentrations of the substituents increase. The total energy plots for $(Mn_{2-x}Fe_x)NiGa$ show that for $x = 0.25$, the martensitic phase is almost destabilized; the ΔE decreases by a factor of more than 3 in comparison to the parent compound. At $x = 0.5$, the tetragonal phase is not even energetically favorable. These are in good agreement with the experimental observations as ΔE is considered as the predictor for T_m [31]. In the case of $Mn_2Ni(Ga_{1-x}Co_x)$, our calculated trends on the composition dependence of the martensitic transformation differs slightly from the experimental observations. In the experiments, no martensitic transformation was observed beyond $x = 0.16$ [32]. Our calculations, on the other hand, obtain a substantially deep energy minimum at $c/a \neq 1$ for $x = 0.25$, signifying the possibility of martensitic transformation at this composition. Qualitatively, though, this result is in agreement with the experimental observation as ΔE gradually decreases with x. The discrepancy can be due to consideration of only the total energy differences. Inclusion of various free-energy contributions can make the deep energy minimum vanish, in agreement with the experiment. We see the same trend of gradual destabilization of the martensitic phases with increasing concentration of the substituents for $(Mn_{2-x}Co_x)NiGa$ and $Mn_2Ni(Ga_{1-x}Fe_x)$ systems. A comparison of the ΔE values for the systems presented in Figs. 3(a) and 3(c) indicates that Co-substituted systems have greater stability of the martensitic phases in comparison to Fe-substituted systems.

In Figs. 3(b) and 3(d), we compare the cases between Fe and Co substitutions, respectively, at the Ni sites. We find a gradual destabilization of the martensitic phase with increasing x for the $Mn_2(Ni_{1-x}Co_x)Ga$ system. A shallow minimum at $c/a \neq 1$ for $x = 0.5$ followed by the absence of any minima for $c/a \neq 1$ for higher x indicate that martensitic transformation at reasonable temperatures might happen for up to $x = 0.25$. This, once again, is slightly different from the experimental observations that no traces of martensitic transformation were obtained for $x > 0.16$ [32]. The case of $Mn_2(Ni_{1-x}Fe_x)Ga$ is somewhat different from the rest. Here, we see a gradual decrease in ΔE with x indicating the gradual destabilization of the martensitic phase up to $x = 0.5$. However, as x increases further, ΔE increases with the highest ΔE obtained for $x = 1$, that is, for the compound Mn_2FeGa. An inspection of the relative volume changes in Table I shows that for this system, the relative changes in volume with x are

substantial and as large as 2.53% for Mn_2FeGa. Thus, although there is a cubic-to-tetragonal transformation, it is not volume conserving and thus is not martensitic in the context of shape memory properties. The physics of cubic-to-tetragonal phase transformation in Mn_2FeGa is very different as discussed in Ref. [71] and thus the trends observed in our calculations do not suggest any anomalous behavior in this system.

A comparison with substituted Ni_2MnGa systems, at this point, is required to understand the similarities and differences between the two systems, in the context of impact of substitutions on the martensitic phase transformation. Unfortunately, there are not enough results available for substituted Ni_2MnGa which discuss the impact of substitution on the phase stability from the point of view of the nature of the energy surfaces as done in Fig. 3. The only work, to our knowledge, is available for Co-substituted Ni_2MnGa [40], where up to 25% of Co was substituted in Ni sites. Comparing our results to Ref. [40], we find that Co doping in Ni_2MnGa strongly affects the equilibrium c/a by gradually reducing it with increase in Co concentration, while there is hardly any change in the equilibrium c/a for the Co-substituted Mn_2NiGa. The reduction in c/a is indeed preferable for obtaining larger MFIS by lowering twinning stress [16] and thus the Co-substituted Ni_2MnGa would be better suited than Co-substituted Mn_2NiGa for actuator applications. A general feature of various substitutions in Mn_2NiGa, as observed in Fig. 3, is that the c/a hardly changes with concentration of the substituent for the compositions where the tetragonal phase is having lower energy than the cubic phase. The only exception is Fe substituted at Ni sites in Mn_2NiGa for high concentrations of Fe. However, in contrast to Co-doped Ni_2MnGa, the equilibrium c/a increases with increasing Fe concentration in $Mn_2(Ni_{1-x}Fe_x)Ga$. Another difference between $(Ni_{1-x}Co_x)_2MnGa$ and $Mn_2(Ni_{1-x}Co_x)Ga$ energy surfaces is in the trends in the barrier height between austenite and martensite phases. While the barrier height decreases with increasing x in the former, the opposite happens in case of the latter. This implies that with increasing concentration of Co substituting Ni, in Mn_2NiGa, the austenite phase gains stability, in accordance with experimental trend. For $Mn_2(Ni_{1-x}Fe_x)Ga$, the change in the barrier heights with x is substantial. For $x = 0.5$ onwards, the barrier height is significantly high which implies that the inverse Heusler structure is gaining metastability with increasing x, and a transformation to a tetragonal structure would require substantial energy. The analysis in terms of the trends in the barrier height, thus, reaffirms that the cubic to tetragonal transformation in $Mn_2(Ni_{1-x}Fe_x)Ga$ for large x is not martensitic in nature.

Figure 3 and the tabulated e/a and ΔE values in Table I now suggest that the ΔE can be considered as a predictor for the qualitative variations in T_m. However, in the systems under consideration, T_m versus e/a correlation is absent except in the $Mn_2(Ni_{1-x}Co_x)Ga$ system, suggesting that e/a would not be a good predictor for T_m. This is consistent with the experimental results [31,32]. Summarizing, we find a universal trend of destabilization of the martensitic phase with increasing Fe or Co concentration, irrespective of the site at which they are substituted. The martensitic phases are stable mostly at low concentrations (up to $x = 0.25$) of the substituent. In the next subsections we analyze the reasons behind this.

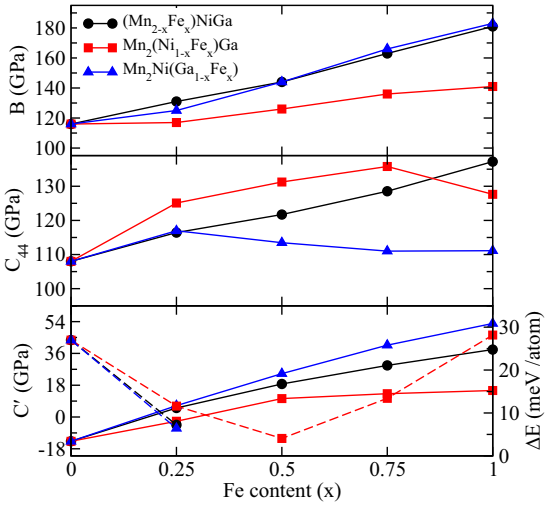

FIG. 4. The calculated bulk modulus B and shear elastic constants C_{44} and C' as a function of Fe content at different sites in Mn_2NiGa. The dashed lines represent variations of ΔE with x; ΔE is defined in Table I.

C. Elastic properties

The composition-dependent variations in the elastic constants of the high-temperature austenite phase having cubic symmetry can often be a predictor of the martensitic transformation for the Ni-Mn-Ga system [38,41]. In Fe, Co, and Cu substituted Ni_2MnGa, it has been established that the shear modulus C' can be a better predictor of composition-dependent T_m [33,39] than e/a since the martensitic transformations in these systems are related to the soft phonon modes which, in turn, are associated with the tetragonal shear elastic constant C' in the high-temperature austenite phase. In Mn_2NiGa, the mechanism of martensitic phase transformation is quite similar to Ni_2MnGa [27]. So the calculation of C' along with other elastic constants would be useful to verify whether C' can be a good predictor of the composition dependence of martensitic transformation apart from the fundamental understanding of the composition dependence of the mechanical stability of these systems.

In Figs. 4 and 5, we present the results of calculated bulk modulus and shear moduli C_{44} and C' for Fe and Co substituted Mn_2NiGa. For all systems, the bulk modulus increases as the volume decreases which is consistent with the expected general trend. The elastic modulus C_{44} is positive for all the alloys which satisfies one of the stability criteria for crystals with cubic symmetry. The value of C' increases with increasing Fe or Co concentration which indicates that the system is increasingly insusceptible to a martensitic transformation. Negative or very low values of C' up to 25% of the substituent concentration for all systems are consistent with the obtained trends in the total energy minima with compositions (Fig. 3). For $Mn_2(Ni_{1-x}Fe_x)Ga$ system, we notice that the C' is almost constant beyond $x = 0.25$ as opposed to the increasing trend (with x) for other systems. This is, once again, consistent with the fact that at all compositions in this particular system, the cubic phase transforms to a tetragonal phase with large energy cost, in particular for $x > 0.5$, although such a phase transformation is not a volume-conserving martensitic one.

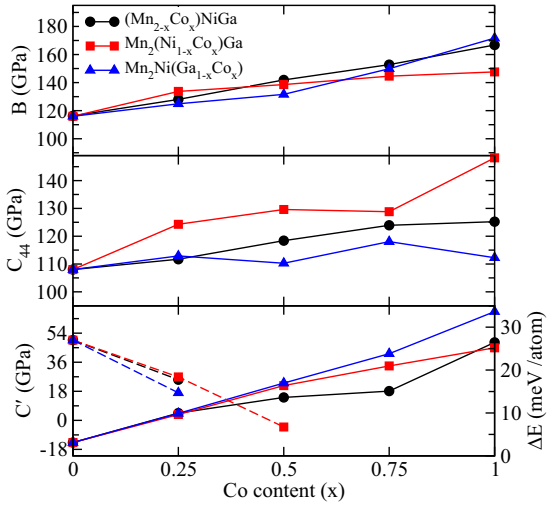

FIG. 5. The calculated bulk modulus B and shear elastic constants C_{44} and C' as a function of Co content at different sites in Mn_2NiGa. The dashed lines represent variations of ΔE with x; ΔE is defined in Table I.

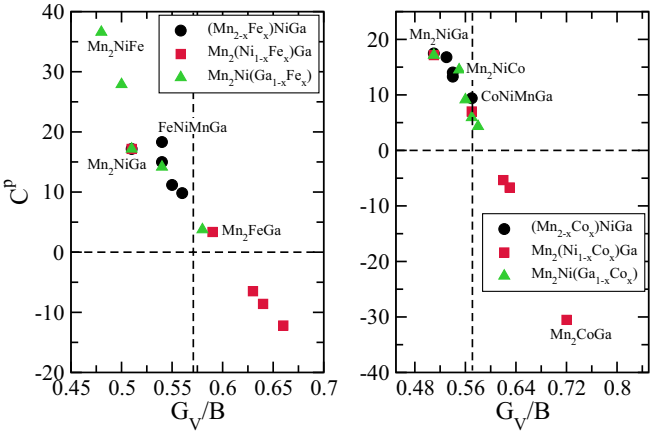

FIG. 6. Variations in the Cauchy pressure $C^p = (C_{12}–C_{44})$ with Pugh ratio G_v/B are plotted for all the compounds. According to Ref. [72], $C^p > 0, G_v/B < 0.57$ indicates more ductility and more components of metallic bonding while $C^p < 0, G_v/B > 0.57$ indicates more brittleness and stronger covalent bonding.

The important outcome of the variations in the C' with compositions is that it can be considered as a better predictor of the composition dependence of T_m. In the previous subsection, we have demonstrated that ΔE is a good predictor of the martensitic transformation. However, in order to fix a predictor, one needs a physically measurable quantity. The justification of considering C' as the one can be understood by looking at the variations of C' with ΔE as shown in Figs. 4 and 5. C' has an inverse relationship with ΔE which is according to our expectations, the former indicating increasing difficulty in destabilizing the Hg_2CuTi structure against tetragonal shear while the latter stands for the possibility of obtaining a martensitic transformation. Another significance of this result is that one can immediately find a similarity with regard to fixing C' as the predictor of the composition dependence of T_m in Fe, Cu, and Co substituted Ni_2MnGa systems. To make sure that this is indeed true in cases of substitutions of all of these three atoms in Mn_2NiGa also, we have plotted the variations of B, C_{44}, and C' with concentration of the substituent for Cu substitution in various sites of Mn_2NiGa (Fig. 1, Ref. [53]) along with variations in ΔE (values taken from Ref. [33]). We see the same inverse relationship between C' and ΔE in this system as well. Thus, we can conclude that C' can be considered as the predictor of the composition dependence of martensitic phase transformation in the Ni-Mn-Ga alloy system, irrespective of substitution by another magnetic atom.

One of the reasons for substituting another magnetic atom into Mn_2NiGa is to improve its mechanical properties, such as ductility. A good measure of whether the system is more ductile or more brittle is to look at its Pugh ratio [73] given as G_v/B [74–76], G_v the isotropic shear modulus under Voigt formalism [77] related to the resistance of the material to plastic deformation and B the bulk modulus. A G_v/B value of 0.57 is considered critical to decide on the brittleness of the compound. Compounds having a Pugh ratio greater than 0.57 are considered more brittle. On the other hand, Cauchy pressure, defined as $C^p = (C_{12}–C_{44})$, provides insight to the nature of bonding in a material with cubic symmetry [78]. According to this, a positive value of Cauchy pressure indicates the presence of more metallic bonding in the system while a negative value implies a stronger component of covalent bonding. Very recently, Niu *et al.* have shown that the Pugh ratio and Cauchy pressure are well correlated with their ductile-to-brittle transition, matching with the metallic-to-covalent bonding transformation for a number of cubic crystals [72]. In Fig. 6, we plot the Pugh ratio versus Cauchy pressure for all the compounds studied here. For better understanding of the trends for each type of substitution, the values of the elastic moduli are given in Table II. The results as displayed in Fig. 6 imply that there is a correlation between C^p and G_v/B as suggested in Ref. [72] and seen in case of a group of Co_2- and Ni_2-based Heusler alloys [76]. However, the absolute numbers in Table II suggest that for a given group of systems, that is, systems obtained by gradual substitution of a particular atom at a particular site of Mn_2NiGa, this correlation does not necessarily hold. For example, one can see a linear variation between C^p and G_v/B in $(Mn_{2-x}Fe_x)NiGa$ for $x \leqslant 0.5$ after which C_p increases with almost no variation in G_v/B. Overall, the results imply that the systems are very close to the ductile-brittle critical limit and that the bonding has a more metallic component; the two notable exceptions are when Co or Fe is substituted at the Ni site. As the Ni content in the system decreases, we observe the tendency of the system to be more brittle and the bonding having a more covalent component. Mn_2CoGa has the highest G_v/B ratio of 0.72 which is close to Si and Ge [72] along with a large negative C^p. The effect is not as dramatic in the case of $Mn_2(Ni_{1-x}Fe_x)Ga$ although a high value of G_v/B, 0.66, along with a C^p value -12.2 are obtained for $x = 0.5$. Beyond $x = 0.5$, the system tends to be more metallic and ductile although the numbers for $x = 0.75$ and 1 are closer to the transition lines. Thus, the bonding features in cases of substitutions at the Ni site must be different from the rest.

TABLE II. Elastic constants of Co and Fe substituted Mn_2NiGa in their Hg_2CuTi cubic phases.

System	B (GPa)	C' (GPa)	C_{44} (GPa)	C_{11} (GPa)	C_{12} (GPa)	G_v (GPa)	G_v/B	$C^p = C_{12}-C_{44}$ (GPa)
Mn_2NiGa	116	−13.75	108	97.67	125.17	59.3	0.51	17.17
$(Mn_{0.75}Fe_{0.25})NiMnGa$	131	5.1	116.43	137.8	127.6	71.9	0.55	11.17
$(Mn_{0.5}Fe_{0.25})NiMnGa$	144	18.69	121.72	168.92	131.54	80.51	0.56	9.82
$(Mn_{0.25}Fe_{0.75})NiMnGa$	163	29.2	128.54	201.93	143.53	88.8	0.54	14.99
FeNiMnGa	181	38.18	137.23	231.91	155.55	97.61	0.54	18.32
Mn_2NiGa	116	−13.75	108	97.67	125.17	59.3	0.51	17.17
$Mn_2(Ni_{0.75}Fe_{0.25})Ga$	117	−2.41	125.1	113.79	118.61	74.1	0.63	−6.49
$Mn_2(Ni_{0.5}Fe_{0.5})Ga$	126	10.42	131.25	139.89	119.05	82.92	0.66	−12.2
$Mn_2(Ni_{0.25}Fe_{0.75})Ga$	136	13.2	135.8	153.6	127.2	86.76	0.64	−8.6
Mn_2FeGa	141	15	127.64	161	131	82.58	0.59	3.36
Mn_2NiGa	116	−13.75	108	97.67	125.17	59.3	0.51	17.17
$Mn_2Ni(Ga_{0.75}Fe_{0.25})$	125	6.44	116.96	133.59	120.71	72.75	0.58	3.75
$Mn_2Ni(Ga_{0.5}Fe_{0.5})$	144	24.56	113.46	176.75	127.63	77.9	0.54	14.17
$Mn_2Ni(Ga_{0.25}Fe_{0.75})$	166	40.66	111	220.21	138.89	82.86	0.5	27.89
Mn_2NiFe	183	52.94	111.12	253.59	147.71	87.85	0.48	36.59
Mn_2NiGa	116	−13.75	108	97.67	125.17	59.3	0.51	17.17
$(Mn_{0.75}Co_{0.25})NiMnGa$	128	4.5	111.71	133.99	125	68.82	0.54	13.29
$(Mn_{0.5}Co_{0.25})NiMnGa$	142	14.21	118.39	160.84	132.43	76.72	0.54	14.04
$(Mn_{0.25}Co_{0.75})NiMnGa$	153	18.11	123.93	176.94	140.73	81.6	0.53	16.8
CoNiMnGa	167	48.27	125.22	231.17	134.62	94.44	0.57	9.4
Mn_2NiGa	116	−13.75	108	97.67	125.17	59.3	0.51	17.17
$Mn_2(Ni_{0.75}Co_{0.25})Ga$	133.7	3.61	124.28	138.51	131.29	76.01	0.57	7.01
$Mn_2(Ni_{0.5}Co_{0.5})Ga$	138.6	21.51	129.61	167.28	124.26	86.37	0.62	−5.35
$Mn_2(Ni_{0.25}Co_{0.75})Ga$	144.6	33.7	128.81	189.54	122.13	90.77	0.63	−6.38
Mn_2CoGa	147.6	44.93	148.18	207.51	117.65	106.88	0.72	−30.53
Mn_2NiGa	116	−13.75	108	97.67	125.17	59.3	0.51	17.17
$Mn_2Ni(Ga_{0.75}Co_{0.25})$	124.9	4.3	112.9	130.63	122.03	69.46	0.56	9.13
$Mn_2Ni(Ga_{0.5}Co_{0.5})$	131.6	23.09	110.28	162.38	116.21	75.4	0.57	5.93
$Mn_2Ni(Ga_{0.25}Co_{0.75})$	149.9	41.29	118.04	204.95	122.37	87.34	0.58	4.33
Mn_2NiCo	171.7	67.36	112.26	261.52	126.79	94.3	0.55	14.53

D. Electronic structure

The results in the previous two subsections demonstrate that the austenite phase gets gradually stabilized as the concentration of the substituent in any one of the sites of Mn_2NiGa increases. For most of the systems investigated, a concentration (of the substituent) beyond 25% leads to a complete stabilization of the cubic austenite phase. At the same time, one sees that except for substitutions at the Ni site, the bonding remains dominantly metallic in nature. In this subsection we try to understand the reasons behind these trends from the composition-dependent variations of the electronic structures in the substituted Mn_2NiGa systems. To do this, we have plotted the total densities of states of compounds where Fe and Co are substituted in various sites. The results for Fe substitution at different sites are shown in Fig. 7 and those for Co substitution at different sites are shown in Fig. 8.

In the Hg_2CuTi phase of pristine Mn_2NiGa, there exists a pseudogap in the minority spin band at about 1 eV below the Fermi level. This pseudogap is formed mainly due to the hybridizations between the $3d$ states of MnI and Ni which occupy symmetric positions in the Hg_2CuTi lattice and the $4p$ states of Ga. A peak around 0.1 eV below Fermi level, originating from the hybridizations of the same orbitals, results in the Jahn-Teller instability in the system [27,58,67,79] and drives the system towards the martensitic transformations. The stabilities of the martensitic phases as obtained from the total energy calculations, the variations in the elastic moduli, and proposed changes in the strengths of bonding upon substitutions can now be interpreted from the minority spin band densities of states. The elastic constant C' is directly connected to the Jahn-Teller distortion since it is the elastic modulus of tetragonal deformation. Thus, a stronger covalent bond or weaker Jahn-Teller distortion should result in a harder C'.

Figures 7 and 8 clearly show that substitutions weaken the Jahn-Teller distortion in Mn_2NiGa as the peak around −0.1 eV gradually gets smeared out, thus stabilizing the Hg_2CuTi structure. This explains the gradual stabilization of the austenite phases with concentrations of the substituents as seen in Fig. 3. Irrespective of the site at which the substitution is done, it is either MnI or Ni content that decreases at the 4a and 4b sites weakening the hybridizations between their $3d$ and Ga $4p$ states. The substituents, either Co or Fe, cannot restore the hybridization as their $3d$ states in the minority bands lie much deeper (Figs. 2 and 3 in Supplemental Material [53]). Such weakening of the Jahn-Teller distortion upon substitutions is

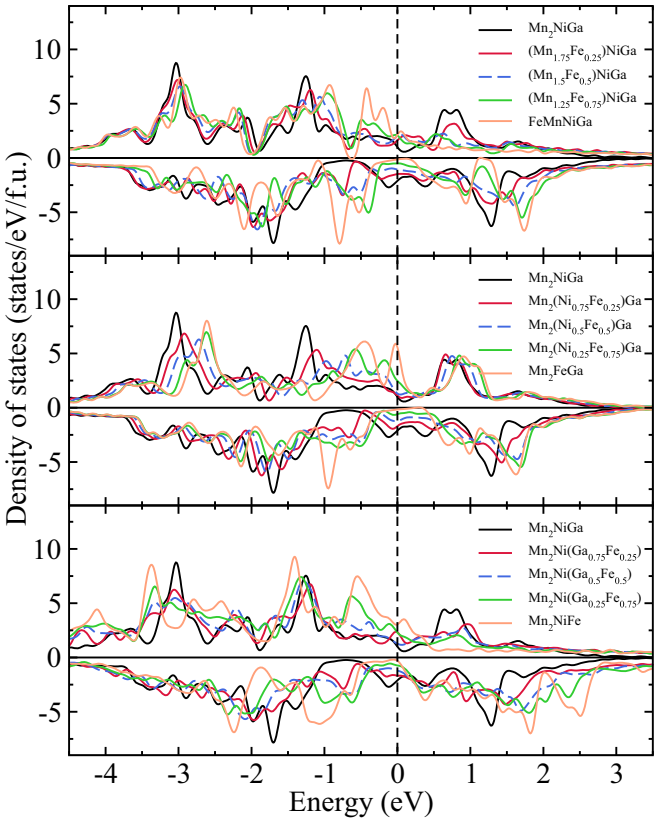

FIG. 7. Total density of states for Fe substituted at different sites in Mn_2NiGa. The zero of the energy is set at Fermi energy (E_F).

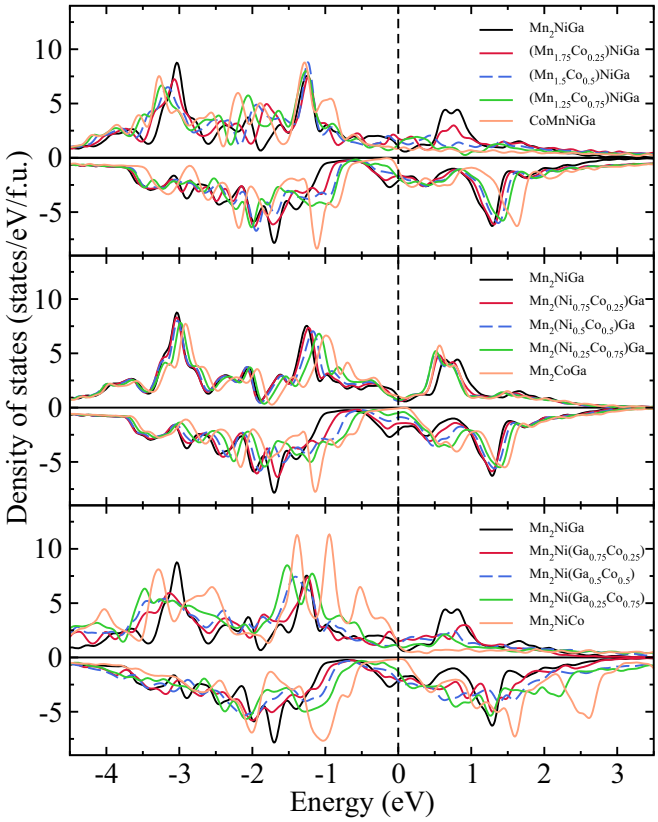

FIG. 8. Total density of states for Co substituted at different sites in Mn_2NiGa. The zero of the energy is set at Fermi energy (E_F).

the reason behind hardening of C' with increasing substituent content in Mn_2NiGa.

As seen from Figs. 7 and 8 as well as Figs. 2 and 3 of the Supplemental Material [53], for the $Mn_{2-x}X_xNiGa$ (X=Fe, Co) systems, the pseudogap at about -1 eV in the minority bands gradually becomes narrower and shallower for X=Fe. This happens primarily due to the position of the Fe-d states which are right in the gap. The weakening of the Jahn-Teller distortion gradually pushes the MnI and Ni states towards lower energies, making them hybridize with Fe states within 0.3 eV to 0.75 eV below Fermi level. Thus, initially for $x \leqslant 0.5$, the covalent bond strength in the system increases and is reflected in the changes in C^p (Table II). Beyond $x = 0.5$, the MnI content reduces weakening the covalent bonding slightly (C^p values increase again along with a decrease in the G_v/B). In the case of X=Co, the situation is slightly different. The Co states lie deeper than Fe states, but the hybridizations with Ni and MnI states which are pushed into the pseudogap due to weakening of the Jahn-Teller effect hybridize with the Co states in a way similar to Fe. The only noticeable difference in the two cases is that while the Fe states are more delocalized towards higher energies, the Co states are localized strengthening the covalent components in the bonding. Such stronger covalent bonding in Co-substituted compounds explains the relative stabilities of the Co-substituted and Fe-substituted compounds as depicted in Fig. 2. In both cases the pseudogap moves towards higher energies but in the case of the Fe substitution it morphs into a real gap cutting through the Fermi level. A look at the majority spin densities of states can also help in understanding the evolution of the bonding strengths. For the Fe-substituted systems, more states pile up near the Fermi level when $x > 0.5$ due to increased hybridization of MnII, Fe, and Ga states contributing to more metallicity in the bonds. In the case of Co substitution at the MnI site, there is very little change in the majority band densities of states and thus the evolution in the bonding nature is to be understood from the features in the minority band densities of states.

In the case of $Mn_2Ni(Ga_{1-x}Fe_x)$, the minority band densities of states are dominated by Fe states weakly hybridizing with other atoms. The Fe states are more delocalized except for $x = 0.25$. However, MnI and Ni hybridize strongly for $x = 0.25$ with the strength gradually diminishing. The majority band densities of states have noticeable changes near the Fermi level with increasing x and beyond $x = 0.25$, the major highlight being a peak and larger densities of states at the Fermi level owing to hybridizations of Fe and MnIII states. This explains the more covalent nature of the bonds for $x = 0.25$ and more metallic for higher x. In the case of $Mn_2Ni(Ga_{1-x}Co_x)$, there is little change in the majority spin densities of states up to $x = 0.75$. In the minority band, Co has greater contributions but it hybridizes weakly with other atoms while the stronger hybridizations are between Ni and MnI in the intermediate concentrations. This means that the covalent bonding gets strengthened supporting the results of Table II. The absence of MnI atoms at $x = 1$, along with sharp

contributions from MnIII near the Fermi level in the majority spin band, weakens the covalent bond strengths and makes the system more metallic.

From Table II, it appears that the substitution at Ni sites makes the covalent bonds stronger and it prevails for Co substitution, in particular. For Co-substituted systems, we find that that there is very little change in the overall features of the majority band densities of states as the Co content increases. The major changes occur in the minority spin band where Co, MnI, and Ni hybridize. As the Ni content decreases, the hybridization between Co and MnI (in the range of -1.25 eV to -0.5 eV) gets stronger making the character of the bonds more covalent. In case of Fe substitution the stronger covalent component in their bonds can be explained in a similar way up to $x = 0.5$. However, at $x = 0.75$, a peak appears close to the Fermi level due to Fe-MnI hybridization, which transforms to a large peak exactly at the Fermi level for $x = 1$, thus increasing the metallic contributions to the bonds. This picture is consistent with the results from Table II.

The electronic structures clearly point out a major difference between substituted Ni_2MnGa and Mn_2NiGa systems. The electronic structures of austenite phases of both the compounds, in their pristine forms, have the pseudogap indicating covalent bonding and the Jahn-Teller peak coming near or at the Fermi level, both occurring due to hybridizations between the elements occupying the 4a, 4b, and 4d sublattices. In Ni_2MnGa the hybridization occurs between Ni and Ga while in Mn_2NiGa, Ni, MnI, and Ga participate in the bonding. In the case of substitutions in Ni_2MnGa, the Jahn-Teller instability is sustained when substitutions are done at the Ga and Mn sites, which is reflected in the increasing height of the Jahn-Teller peak at the Fermi level [39]. This correlates well with the experimental observation of the increase in T_m with increasing concentration of the substituent. The substitutions at Ni sites in Ni_2MnGa, on the other hand, lead to gradual lowering of the height of the Jahn-Teller peak [39,40] signifying increasing stability of the austenite phase and subsequent decrease in T_m. The sustaining Jahn-Teller instability for cases where substitutions are done at Ga and Mn sites is due to the fact that Ni is not involved in these cases. The substitutions at the Ni sites weaken the Ni-Ga hybridizations and relieve the Jahn-Teller instability. Substitutions at any of the three sites (MnI, Ni, and Ga) of Mn_2NiGa diminish the Jahn-Teller effect as all three atoms are involved in producing the peak associated with it. Thus, irrespective of the site of substitution, we see the manifestation of decreasing Jahn-Teller effect by reduction in the peak height at or near the Fermi level with increasing concentration of the substituent. This explains why T_m decreases with substitution at any site in Mn_2NiGa while this is not the case for substituted Ni_2MnGa. Another distinctive outcome of substitutions in Mn_2NiGa is the emergence of a half-metal-like gap which grows as the concentration of the substituent increases and finally cuts through the Fermi level when substitution is complete ($x = 1$) producing materials with high spin polarization, which could be useful in spintronics. This is very different from what is obtained in substituted Ni_2MnGa. While the substitutions in both the systems fill the pseudogap in the minority band, thus making it narrow, in the case of Mn_2NiGa, the substitutions diminish the Jahn-Teller peaks considerably as either MnI, Ni, or Ga content is reduced. Along with this, the positions of the substituent levels are deep within the minority band, producing a gap across the Fermi level. This is not the case for substituted Ni_2MnGa.

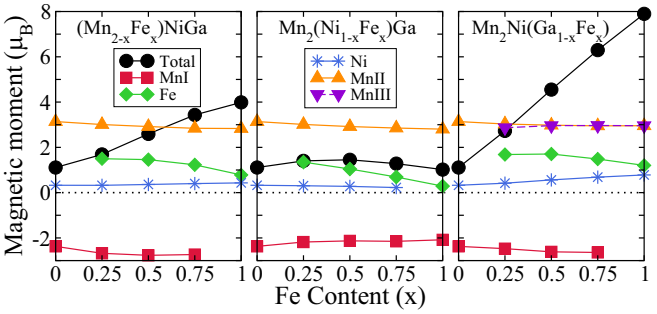

FIG. 9. The calculated total (μ_B/f.u.) and atomic magnetic moment as a function of Fe content for Fe-substituted Mn_2NiGa.

E. Total and atomic magnetic moments

In Table I and Figs. 9 and 10 we present our results on total and atomic magnetic moments to understand the effects of site substitution in Mn_2NiGa in the Hg_2CuTi phase. Magnetization measurements on $(Mn_{2-x}Fe_x)NiGa$ [31], $Mn_2(Ni_{1-x}Co_x)Ga$, and $Mn_2Ni(Ga_{1-x}Co_x)$ [32] systems showed an increase in magnetization upon Fe and Co substitutions. From our results, we summarize the observations on the total magnetic moments: (i) In almost all cases the total moment increases with the concentration of the substituent. (ii) The rise in the total moment is fastest for $Mn_2Ni(Ga_{1-x}X_x)$ and is slowest for $Mn_2(Ni_{1-x}X_x)Ga$ systems. (iii) The variation of total moment with x is nonlinear for $Mn_2(Ni_{1-x}Fe_x)Ga$. It increases for $x \leqslant 0.5$ and then decreases for higher values of x. However, this is consistent with the substantial changes in the electronic structures discussed in the previous subsection. (iv) All the compounds formed by complete substitution of one of the atoms in the parent compound ($x = 1$) have near-integer moments with the highest being $\sim 9\ \mu_B$ for Mn_2NiCo.

The calculated results agree very well with the ones available in the literature, obtained either in the magnetic measurements [31,32] or from the first-principles calculations [33,43,68,69]. For $(Mn_{2-x}Fe_x)NiGa$ ($x = 0.25, 0.5$) compounds, the calculated results of magnetic moments are consistent with experiment [31]. The noticeable disagreements

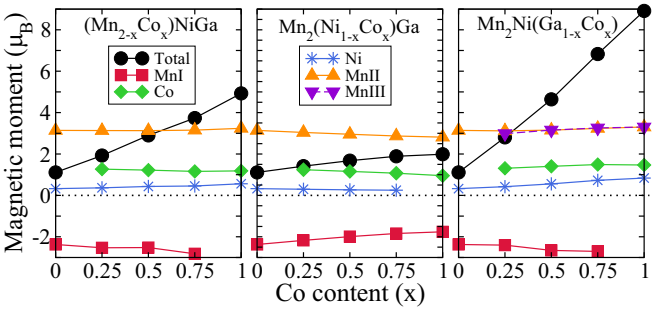

FIG. 10. The calculated total (μ_B/f.u.) and atomic magnetic moment as a function of Co content for Co-substituted Mn_2NiGa.

are in the cases of $Mn_2Ni(Ga_{1-x}Co_x)$ ($x = 0.25,0.5$) [32], MnCoNiGa [18,43], and MnFeNiGa [43] compounds. The disagreement in the case of $Mn_2Ni(Ga_{1-x}Co_x)$ could be because of the presence of antisite disorder in the experimental sample or due to the differences between actual composition and the one reported in the experiment [32]. Both the effects can affect the magnetic moment as it is found to be very sensitive to the sublattice composition in Ni-Mn-Ga systems [39]. The cases of MnCoNiGa and MnFeNiGa are quite insightful. DFT calculations on both compounds with a stacking identical to that obtained by replacing MnI with Co or Fe is in excellent agreement with our results [43], both producing near-integer moments and a half-metal-like gap in the minority band densities of states. However, the magnetization measurements at low temperature obtained saturation moments which are far from being integers [43]. The same compounds can be obtained by substituting Co or Fe at Ni sites in Ni_2MnGa. Magnetization measurements and DFT calculations for Co-substituted Ni_2MnGa compound with equal amounts of Co, Ni, Mn, and Ga reported noninteger magnetic moments [18] with values in excellent agreement with the experimental results reported in Ref. [43]. The origin of such discrepancies, probably, is in the differences in the site preferences if one obtains the same compounds by substitutions in Mn_2NiGa and in Ni_2MnGa. In the case of the former, we have explained why the stacking is Co(4a)-MnII(4c)-Ni(4b)-Ga(4d) in Sec. III A. This comes out to be the minimum energy stacking for CoNiMnGa [43]. In the case of substitutions of Co at the Ni sites in Ni_2MnGa, the expected stacking would be (Ni-Co)(4a)-Mn(4c)-(Ni-Co)(4b)-Ga(4d). This is because, in Heusler Ni_2MnGa, the Ni sites are crystallographically equivalent, and thus the substituent Co would not prefer one Ni site over the other and would occupy both in equal proportions keeping the symmetry of the lattice intact. The noninteger magnetic moment as obtained experimentally and by DFT calculations [18] must be due to this. This might be true in the case of magnetization measurements in quaternary MnCoNiGa and MnFeNiGa, although they are not obtained by the above-mentioned substitution route. One needs to investigate the energetics associated with different site occupancies in these compounds to resolve the issue. The importance of the observed discrepancy in CoNiMnGa magnetic moment is in establishing that the site substitutions and subsequent properties can be very different in the two pristine compounds.

The changes in the compositions at various sites affect the atomic moments which in turn affect the variations in the total magnetic moments with the concentration of the substituents. From Figs. 9 and 10, we find the following trends: (i) Like Mn_2NiGa, MnI and MnII atoms couple antiparallel in all compounds where MnI is present. (ii) The moment of MnII atoms undergoes little variation with the composition across all compounds, the general trend being a small decrease with the concentration of the substituent. (iii) The moment associated with the Ni atoms increases with concentration of the substituent except when it is substituted by Fe or Co; the faster increase is in cases of substitutions at Ga sites. (iv) The MnI magnetic moments increase slightly in magnitude making the antiferromagnetic component in the system stronger as the concentration of the substituent increases for all systems except when substitutions are done at Ni sites, where its magnitude decreases signifying increase in the ferromagnetic component in the system; the change is more rapid in the case of Co substitution at the Ni site. (v) For the Ga-substituted systems, MnIII, the Mn atoms at the Ga sites have large ferromagnetic moments, almost equal in magnitude to MnII moments; as the concentration of the substituent increases the concentration of MnI (MnIII) decreases (increases) weakening the antiferromagnetic component in favor of a strong ferromagnetic one. This explains the rapid increase of the total moment for these systems. (vi) The Co moment is larger than the Ni moment and undergoes little change across compositions and the site of substitution while the Fe moment has a general trend of decreasing with increasing Fe concentration. A rapid quenching of Fe moment is observed in the case of Mn_2FeGa, the reason of which has been discussed earlier [71]. The slow increase in the total moment for Ni-substituted systems, thus, can be understood in terms of the losses of MnII and MnI moments concurrently but in opposite directions, leaving the changes to be governed solely by Ni and the substituent moments, both of which vary slowly across compositions. The linear increase in the total moment of the Mn-substituted system, on the other hand, can be attributed to the gradual loss of contributions of MnI due to its decreasing concentration which boosts the ferromagnetic component in the system with concentration of the substituent. The explanations on the nature of such variations in the atomic moments require analysis of the electronic structures of each constituent. This has been done in Ref. [53].

F. Magnetic exchange interactions and Curie temperature

In Figs. 11 and 12, we show the composition dependencies of Curie temperatures (T_c) calculated using the mean-field approximation (MFA) and Monte Carlo simulation (MCS), respectively, for Fe and Co substituted Mn_2NiGa. Since the MFA results typically overestimate the T_c and MCS results are found to be closer to experimental results for a variety of systems, the available experimental results in these compounds are included in Fig. 12. The trends in variations of T_c calculated using MFA and MCS are by and large similar. As expected, the MFA results are overestimated in comparison with the MCS results and the experimental values. From the MCS

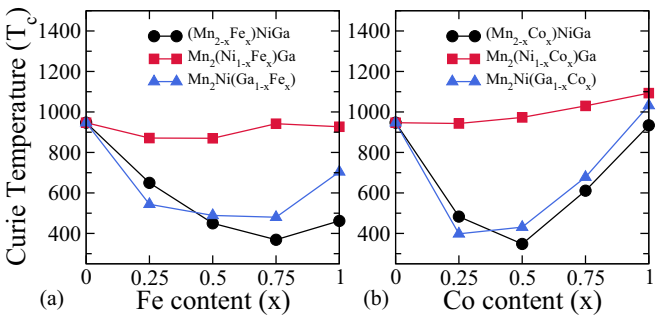

FIG. 11. Calculated Curie temperatures as a function of substituent (a) Fe concentration and (b) Co concentration for substitutions at different sites in Mn_2NiGa. Calculations are done by the MFA method.

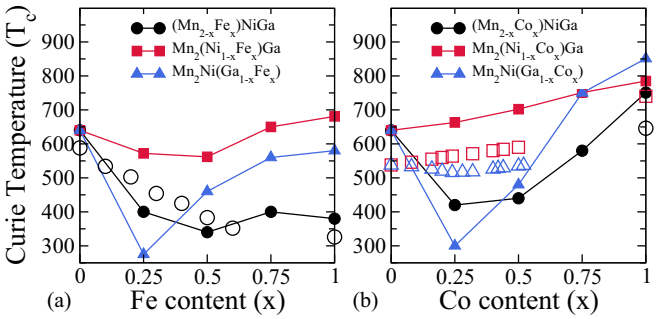

FIG. 12. Calculated Curie temperatures as a function of substituent (a) Fe concentration and (b) Co concentration for substitutions at different sites in Mn_2NiGa. Calculations are done by the MCS method. Open symbols represent the experimental results which are adopted from Refs. [31,32,43,80].

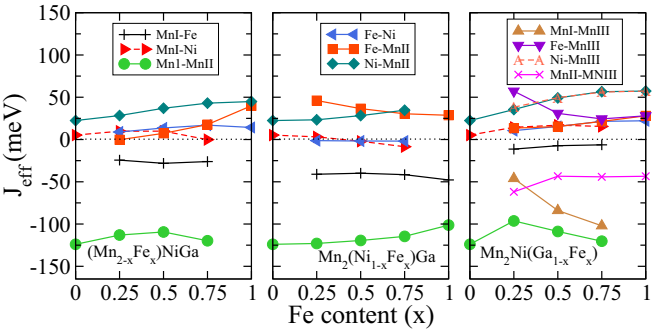

FIG. 13. Effective exchange coupling constant (J_{eff}) as a function of Fe content at different sites in Mn_2NiGa.

results, we find that all the end compounds obtained by complete substitution of Fe or Co in any of the sites have very high T_c, the largest being close to 900 K for Mn_2NiCo. The qualitative variation of T_c for $Mn_2(Ni_{1-x}Co_x)Ga$ agrees well with the experiment [32,80] although the MCS results are a little overestimated. The quantitative agreement between the MCS results and the experimental results [31,43] for $(Mn_{2-x}Fe_x)NiGa$ is better. There is significant disagreement, both qualitatively and quantitatively, for $Mn_2Ni(Ga_{1-x}Co_x)$ systems. The MCS calculations show a sharp decrease in T_c for 25% Co substitution after which the T_c rises sharply with increase in x. For the experiment [32], on the other hand, although a decrease in T_c up to $x = 0.24$ and a rise after that were obtained, the changes were not this substantial. The experimentally obtained T_c decreased from 538 K ($x = 0$) to 517 K for $x = 0.24$ and rose to only 537 K for $x = 0.52$. It may be noted that their T_c for Mn_2NiGa is lower by 50 K in comparison to T_c obtained from other experiments [25,31]. Such discrepancies could be due to antisite disorder or off-stoichiometric compositions present in the samples used by the authors of Ref. [32]. In fact, we have reported discrepancies in the magnetic moments calculated by us and obtained from their magnetic measurements in the previous subsection. Thus the origin of these discrepancies could be the same. Nevertheless, the agreement between the MCS results and the experiments for the end compounds, wherever available, is remarkable.

In order to understand the trends in the Curie temperature, we have calculated the interatomic magnetic effective exchange coupling (J_{eff}), presented in Figs. 13 and 14 for Fe and Co substituted Mn_2NiGa, respectively. The J_{eff} are calculated as $J_{\text{eff}}^{\mu\nu} = \sum_j J_{0j}^{\mu\nu}$, 0 fixed to sublattice μ and the sites j belonging to sublattice ν. We find that the dominant J_{eff}'s remain either antiferromagnetic or ferromagnetic across compositions. The dominant antiferromagnetic J_{eff} is due to the MnI-MnII pairs while the other dominant inter-sublattice J_{eff}'s are ferromagnetic. For the $(Mn_{2-x}Co_x)NiGa$ system, the strength of antiferromagnetic $J_{\text{eff}}^{\text{MnI-MnII}}$ decreases with x while the strength of the largest ferromagnetic effective exchange interaction, $J_{\text{eff}}^{\text{Co-MnII}}$, increases with x. This is because of the increasing hybridizations between nearest-neighbor Co and MnII which couple parallel resulting in the weakened antiferromagnetic nearest-neighbor MnI-MnII exchange interaction as the system gradually becomes MnI deficient (Co excess). The increasing ferromagnetic exchange interaction between nearest-neighbor Ni and MnII and next-nearest-neighbor Ni-MnI and Ni-Co gives rise to an increase in the overall ferromagnetic interaction. Up to $x = 0.25$, there is a competition between the ferromagnetic and antiferromagnetic interactions which brings T_c down. Beyond $x = 0.25$, the ferromagnetic components overwhelm the antiferromagnetic interactions resulting in the rise of T_c for higher values of x. In contrast, for $(Mn_{2-x}Fe_x)NiGa$, the $J_{\text{eff}}^{\text{MnI-MnII}}$ remains nearly constant with x. The strengths of the ferromagnetic Fe-MnII, Fe-Ni, and MnI-Ni in these compounds are weaker in comparison to those in $(Mn_{2-x}Co_x)NiGa$ with the Ni-MnII exchange interaction having nearly the same strengths and larger than the Fe-MnII one, exactly opposite to the Co-substituted compound. Such weaker ferromagnetic interactions are artifacts of weaker Fe-MnII hybridizations, particularly for low values of x as can be seen from the atom-projected densities of states (Fig. 2 of the Supplemental Material [53]) which shows that the major peaks of Fe and MnII are always separated. This weak interaction of MnII with one of the components in the 4a site keeps the strength of the interaction with the other component, MnI, at the same site intact across compositions although the concentration of MnI decreases gradually. This manifests itself in bringing down the T_c considerably in $(Mn_{2-x}Fe_x)NiGa$ for low x and keeping it almost like that as x increases.

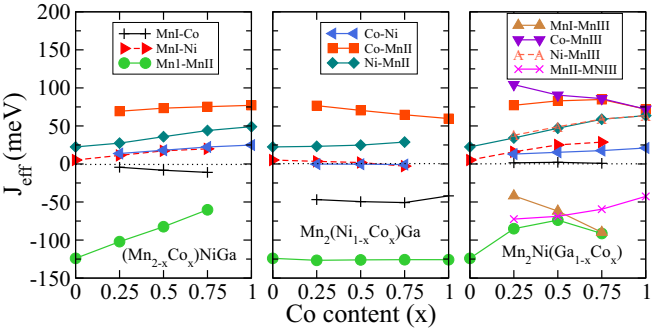

FIG. 14. Effective exchange coupling constant (J_{eff}) as a function of Co content at different sites in Mn_2NiGa.

For $Mn_2(Ni_{1-x}Co_x)Ga$ and $Mn_2(Ni_{1-x}Fe_x)Ga$, we find the variations in the exchange interactions quite similar, qualitatively and quantitatively. The antiferromagnetic MnI-MnII interactions remain largely unaffected across compositions as the substitutions are not done in either of these sites. The inter-sublattice antiferromagnetic MnI-Fe and MnI-Co second-neighbor interactions are found to be substantial and identical in strengths. The strongest ferromagnetic interaction in the Co-substituted system is that of Co-MnII pairs while the strength of the Ni-MnII interaction is considerably weaker across the concentration range. In the case of Fe-substituted system, though the strongest ferromagnetic interaction is due to Fe-MnII pairs for smaller x values, the strength of Ni-MnII interactions quickly catches up with it. This is because of weakened hybridizations between Fe and MnII (Fig. 2 of the Supplemental Material [53]) as x increases. Thus, the initial decrease in T_c for $Mn_2(Ni_{1-x}Fe_x)Ga$ is due to weakening of the overall ferromagnetic interactions, primarily due to weak Fe-MnII hybridizations. For higher x, the $J_{\text{eff}}^{\text{Ni-MnII}}$ compensates for the $J_{\text{eff}}^{\text{Fe-MnII}}$, strengthening the ferromagnetic interactions in the system leading to an increase in T_c with x. For $Mn_2(Ni_{1-x}Co_x)Ga$, the strong ferromagnetic exchange interactions for all x values lead to an increase in T_c with x.

In systems with substitutions done at Ga sites, a greater number of interactions compete with each other as Mn atoms are present at three different sites. The antiferromagnetic interactions are due to nearest neighbors MnI-MnII and MnI-MnIII and second neighbor MnII-MnIII. The ferromagnetic components in the exchange interactions are due to nearest neighbors X-MnIII (X=Co, Fe), X-MnII, Ni-MnII, and Ni-MnIII and second neighbor Ni-MnI. For X=Co, that is, when Ga is replaced with Co, the antiferromagnetic MnI-MnII interaction loses its strength as does the second-neighbor antiferromagnetic MnII-MnIII interaction while the nearest-neighbor MnIII-MnI interaction becomes more antiferromagnetic as concentration of Co increases. Among the ferromagnetic interactions, except for Co-MnIII which decreases with concentration of Co, the other three increase. Strong hybridizations of Co with MnII and MnIII atoms are responsible for the strong ferromagnetic interactions in this system. This was predicted earlier [32] without explicit computations of the exchange interactions. Our calculation corroborates this with quantitative estimates. The antiferromagnetic exchange interactions behave the same way in systems with X=Fe. The ferromagnetic components for Fe-substituted system are much weaker than those for Co-substituted systems. In fact, although Fe-MnIII was the strongest ferromagnetic interaction initially, it drops fast giving way to Ni-MnII and Ni-MnIII. Weaker hybridizations between Fe and Mn-II/Mn-III as Fe concentration increases can easily be seen from the atomic densities of states (Fig. 2 of the Supplemental Material [53]). As Fe concentration increases, the Fe majority spin states move towards higher energies in comparison with MnII/MnIII states, thus making the hybridizations weaker. The weaker ferromagnetic components in Fe-substituted systems explain their smaller T_c values, in comparison to Co-substituted systems, particularly for higher x values. In both systems, the sharp decrease at $x = 0.25$ is due to relatively stronger antiferromagnetic interactions. As x increases, the ferromagnetic interactions build up, effecting an increase in T_c.

IV. SUMMARY AND CONCLUSIONS

With the help of first-principles density functional theory based calculations, we perform an in depth investigations of the effects of Fe and Co substitutions in magnetic shape memory system Mn_2NiGa. We study the site preferences of the substituents, the stabilities of the substituted compounds, and their various properties in order to understand different aspects of substitutions in Mn_2NiGa, which in combination with available results on the Ni_2MnGa systems with similar substitutions can provide a consistent picture of the effects of such substitution in Ni-Mn-Ga alloys. We perform investigations mostly in the Hg_2CuTi structure which represents the high-temperature austenite phase of Mn_2NiGa. Regarding site preferences and stability of the compounds formed by substitutions at different sites, we find that the substituents prefer the sites of substituting atoms when Ni or Mn is being substituted. In the case of substitution of Ga, the substituents prefer to occupy the 4a sites in the Hg_2CuTi lattice, displacing the original constituent to the 4d site. This is in contrast with substituted Ni_2MnGa where site preferences sensitively depend on the substituting site and the substituent. We also find that the Co substitution in Mn_2NiGa makes the system more stable in comparison to Fe-substituted Mn_2NiGa.

The patterns in the site occupancies lead to a gradual stabilization of the austenite phase of Mn_2NiGa irrespective of the site of substitution and the substituent, in agreement with experimental observations [31,32]. This uniform trend is an artifact of progressive weakening of the Jahn-Teller distortion that drives martensitic transformation in Mn_2NiGa. The Jahn-Teller instability in the Hg_2CuTi phase of Mn_2NiGa is due to the hybridizations between the d states of constituents at the 4a and 4b positions(MnI and Ni, respectively) and the p states of Ga in the minority band. Since the substitution of another transition-metal element such as Fe or Co in Mn_2NiGa invariably replaces the elements at the 4a and 4b positions, the hybridizations leading to the Jahn-Teller instability gradually vanish with the increase in concentration of the substituent. The deep-lying states of Fe and Co cannot restore the Jahn-Teller instability, but rather contribute to its decline. The fact that the strengthening (weakening) of the Jahn-Teller distortion upon substitution can explain the gradual stabilization of the martensite (austenite) phase is also seen in the case of substituted Ni_2MnGa [39,40]. However, the differences in the electronic structures in the two substituted systems, stemming from the differences in the stacking sequence of the atoms in their respective austenite phases, lead to different trends in the stabilizations of the austenite phases as a function of substituent concentration. Thus, the site preferences of the substituents along with the positions of their states inside the minority spin bands can help understand the trends in the phase stability of Ni-Mn-Ga alloys over a large composition range.

The results on elastic moduli provide two useful pieces of information: (i) the tetragonal shear modulus C' can be considered as a predictor of the martensitic transformation and (ii) a correspondence between the ductile-to-brittle and metallic-to-covalent bonding transition can be curved out for substituted Mn_2NiGa. We find that the weakening of the Jahn-Teller instability largely correlates with the strengthening of

the covalent bonds, due to hybridizations of the minority spin states of the substituents with either of the elements in 4a and 4b positions along with Ga at the 4d sites. The substitution at Ni sites renders the systems more covalent as well as more brittle, while the rest of the systems are, by and large, more metallic and ductile.

An immediate consequence of the disappearance of the Jahn-Teller distortion and the positions of the energy levels of the substituents which are deeper into the occupied parts of the minority spin bands of Mn_2NiGa is the opening of an energy gap in the minority band cutting through the Fermi level. This gap is like a half-metallic gap with spin polarizations of the substituted Mn_2NiGa reaching near 100% when the substitution is complete. We find that all the compounds formed by 100% substitution have nearly integer magnetic moment and nearly follow the Slater-Pauling rule of $M = N_v - 24$ [81,82], with M the total magnetic moment and N_v the number of valence electrons. Thus Fe and Co substitutions, although leaving Mn_2NiGa unsuitable for shape memory applications except at low concentrations of the substituents, produce compounds which are potentially useful for other magnetic applications. This is in contrast to the substituted Ni_2MnGa, where Fe and Co substitutions at Mn and Ni sites lead to compounds Ni_2CoGa, Ni_2FeGa, NiCoMnGa, and NiFeMnGa; the first two are shape memory materials and the last two are normal metals.

The magnetic properties of Mn_2NiGa in general improve with more presence of the substituents. This is because of increasing ferromagnetic exchange interactions between the substituents and other magnetic atoms, and subsequent weakening of the dominant MnI-MnII antiferromagnetic interaction. The magnetic moments increase with concentration of the substituents as a result of this, the highest rise being in the case of substitutions at the Ga sites, where an uncommon pattern of site occupancy magnifies ferromagnetic exchange interactions. Thus, we find a stable magnetic material Mn_2NiCo with a moment as high as $\sim 9\,\mu_B$/f.u. The magnification of ferromagnetic exchange interactions elevates the Curie temperatures in these systems with T_c of Mn_2NiCo as high as $\sim$900 K. This material is in the league of newly discovered magnets in the Heusler family having only 3d transition metals as their components [44]. The presence of competing antiferromagnetic and ferromagnetic exchange interactions in all the compounds studied here gives rise to nonmonotonic variations in T_c, in stark contrast to substituted Ni_2MnGa compounds where T_c varies rather monotonically with the concentration of the substituents [18,83]. Such monotonic variations in substituted Ni_2MnGa are due to the fact that unlike substituted Mn_2NiGa, the dominant exchange interactions are ferromagnetic, and thus T_c is controlled by the variations in particular ferromagnetic interactions with concentration of the substituents.

In conclusion, this work has explored the interrelations between the site occupancy, martensitic phase stability, bonding picture, and mechanical and magnetic properties of Fe and Co substituted Mn_2NiGa. The results demonstrate that the same analytical approach can be used for substituted Ni_2MnGa and Mn_2NiGa and thus the effects of substitution of another transition metal in the Ni-Mn-Ga system over a wide range of composition can be easily predicted. However, knowledge of the physical mechanisms in substituted Ni_2MnGa cannot be rigidly applied to predict the trends in properties of substituted Mn_2NiGa compounds as there are significant differences between the two pristine compounds starting with their crystal structures. This work is a comprehensive investigation of the similarities and differences between the impacts of substitutions in these two systems and analysis of them from a microscopic point of view. An important and somewhat unexpected outcome of this work is the emergence of highly spin-polarizable, nearly half-metallic compounds with high Curie temperatures upon complete substitution. The material Mn_2NiCo shows promise with its very high moment, spin polarization, and T_c. These results can motivate experimentalists to explore such materials. This work also acts as a guide to researchers on the choice of suitable substituent and composition to improve functional properties of Ni-Mn-Ga systems.

ACKNOWLEDGMENT

The authors would like to thank IIT Guwahati and Department of Science and Technology, India (Grant No. SR/FST/P-II/020/2009) for the PARAM supercomputing facility and the computer cluster in the Department of Physics, IIT Guwahati

[1] K. Ullakko, J. Huang, C. Kantner, R. O'Handley, and V. Kokorin, Appl. Phys. Lett. **69**, 1966 (1996).
[2] S. J. Murray, M. Marioni, S. M. Allen, R. C. O'Handley, and T. A. Lograsso, Appl. Phys. Lett. **77**, 886 (2000).
[3] A. Sozinov, A. Likhachev, N. Lanska, and K. Ullakko, Appl. Phys. Lett. **80**, 1746 (2002).
[4] M. Chmielus, X. Zhang, C. Witherspoon, D. Dunand, and P. Müllner, Nat. Mater. **8**, 863 (2009).
[5] J. Marcos, A. Planes, L. Mañosa, F. Casanova, X. Batlle, A. Labarta, and B. Martínez, Phys. Rev. B **66**, 224413 (2002).
[6] F.-x. Hu, B.-g. Shen, J.-r. Sun, and G.-h. Wu, Phys. Rev. B **64**, 132412 (2001).
[7] T. Krenke, E. Duman, M. Acet, E. F. Wassermann, X. Moya, L. Mañosa, A. Planes, E. Suard, and B. Ouladdiaf, Phys. Rev. B **75**, 104414 (2007).
[8] M. Pasquale, C. P. Sasso, L. H. Lewis, L. Giudici, T. Lograsso, and D. Schlagel, Phys. Rev. B **72**, 094435 (2005).
[9] C. Biswas, R. Rawat, and S. Barman, Appl. Phys. Lett. **86**, 202508 (2005).
[10] B. Ingale, R. Gopalan, V. Chandrasekaran, and S. Ram, J. Appl. Phys. **105**, 023903 (2009).
[11] A. Planes, L. Mañosa, and M. Acet, J. Phys.: Condens. Matter **21**, 233201 (2009).
[12] A. Likhachev, A. Sozinov, and K. Ullakko, Mater. Sci. Eng. A **378**, 513 (2004).
[13] A. Sozinov, A. Likhachev, and K. Ullakko, IEEE Trans. Magn. **38**, 2814 (2002).
[14] P. Webster, K. Ziebeck, S. Town, and M. Peak, Philos. Mag. B **49**, 295 (1984).
[15] L. Pareti, M. Solzi, F. Albertini, and A. Paoluzi, Eur. Phys. J. B **32**, 303 (2003).

[16] A. Sozinov, N. Lanska, A. Soroka, and W. Zou, Appl. Phys. Lett. **102**, 021902 (2013).

[17] D. Soto, F. A. Hernández, H. Flores-Zúñiga, X. Moya, L. Mañosa, A. Planes, S. Aksoy, M. Acet, and T. Krenke, Phys. Rev. B **77**, 184103 (2008).

[18] T. Kanomata, Y. Kitsunai, K. Sano, Y. Furutani, H. Nishihara, R. Y. Umetsu, R. Kainuma, Y. Miura, and M. Shirai, Phys. Rev. B **80**, 214402 (2009).

[19] T. Kanomata, T. Nozawa, D. Kikuchi, H. Nishihara, K. Koyama, and K. Watanabe, Int. J. Appl. Electromagn. Mech. **21**, 151 (2005).

[20] A. Gomes, M. Khan, S. Stadler, N. Ali, I. Dubenko, A. Takeuchi, and A. Guimarães, J. Appl. Phys. **99**, 08Q106 (2006).

[21] M. Khan, I. Dubenko, S. Stadler, and N. Ali, J. Appl. Phys. **97**, 10M304 (2005).

[22] T. Kanomata *et al.*, Metals **3**, 114 (2013).

[23] D. Soto-Parra *et al.*, Philos. Mag. **90**, 2771 (2010).

[24] T. Kanomata, S. Nunoki, K. Endo, M. Kataoka, H. Nishihara, V. V. Khovaylo, R. Y. Umetsu, T. Shishido, M. Nagasako, R. Kainuma, and K. R. A. Ziebeck, Phys. Rev. B **85**, 134421 (2012).

[25] G. Liu *et al.*, Appl. Phys. Lett. **87**, 262504 (2005).

[26] G. D. Liu, X. F. Dai, S. Y. Yu, Z. Y. Zhu, J. L. Chen, G. H. Wu, H. Zhu, and J. Q. Xiao, Phys. Rev. B **74**, 054435 (2006).

[27] A. Kundu, M. E. Gruner, M. Siewert, A. Hucht, P. Entel, and S. Ghosh, Phys. Rev. B. **96**, 064107 (2017).

[28] S. Singh, M. Maniraj, S. D'Souza, R. Ranjan, and S. Barman, Appl. Phys. Lett. **96**, 081904 (2010).

[29] P. J. Brown, T. Kanomata, K. Neumann, K. U. Neumann, B. Ouladdiaf, A. Sheikh, and K. R. A. Ziebeck, J. Phys.: Condens. Matter **22**, 506001 (2010).

[30] S. Singh, S. Esakki Muthu, A. Senyshyn, P. Rajput, E. Suard, S. Arumugam, and S. Barman, Appl. Phys. Lett. **104**, 051905 (2014).

[31] H. Luo *et al.*, J. Appl. Phys. **107**, 013905 (2010).

[32] L. Ma, W. H. Wang, C. M. Zhen, D. L. Hou, X. D. Tang, E. K. Liu, and G. H. Wu, Phys. Rev. B **84**, 224404 (2011).

[33] A. Chakrabarti, M. Siewert, T. Roy, K. Mondal, A. Banerjee, M. E. Gruner, and P. Entel, Phys. Rev. B **88**, 174116 (2013).

[34] E. C. Do, Y.-H. Shin, and B.-J. Lee, Calphad **32**, 82 (2008).

[35] V. Ramamurthy and S. Rajendraprasad, J. Phys. Chem. Solids **47**, 1109 (1986).

[36] D. Winder and C. S. Smith, J. Phys. Chem. Solids **4**, 128 (1958).

[37] Q.-M. Hu, C.-M. Li, R. Yang, S. E. Kulkova, D. I. Bazhanov, B. Johansson, and L. Vitos, Phys. Rev. B **79**, 144112 (2009).

[38] C.-M. Li, H.-B. Luo, Q.-M. Hu, R. Yang, B. Johansson, and L. Vitos, Phys. Rev. B **82**, 024201 (2010).

[39] C.-M. Li, H.-B. Luo, Q.-M. Hu, R. Yang, B. Johansson, and L. Vitos, Phys. Rev. B **84**, 024206 (2011).

[40] M. Zelený, A. Sozinov, L. Straka, T. Björkman, and R. M. Nieminen, Phys. Rev. B **89**, 184103 (2014).

[41] S. Ghosh, L. Vitos, and B. Sanyal, Phys. B: Condens. Matter **406**, 2240 (2011).

[42] S. R. Barman, A. Chakrabarti, S. Singh, S. Banik, S. Bhardwaj, P. L. Paulose, B. A. Chalke, A. K. Panda, A. Mitra, and A. M. Awasthi, Phys. Rev. B **78**, 134406 (2008).

[43] V. Alijani, J. Winterlik, G. H. Fecher, S. S. Naghavi, and C. Felser, Phys. Rev. B **83**, 184428 (2011).

[44] S. Sanvito *et al.*, Sci. Adv. **3**, e1602241 (2017).

[45] P. E. Blöchl, Phys. Rev. B **50**, 17953 (1994).

[46] G. Kresse and J. Furthmüller, Phys. Rev. B **54**, 11169 (1996).

[47] G. Kresse and D. Joubert, Phys. Rev. B **59**, 1758 (1999).

[48] J. P. Perdew, K. Burke, and M. Ernzerhof, Phys. Rev. Lett. **77**, 3865 (1996).

[49] M. Methfessel and A. T. Paxton, Phys. Rev. B **40**, 3616 (1989).

[50] F. Murnaghan, Proc. Natl. Acad. Sci. USA **30**, 244 (1944).

[51] L. Vitos, *Computational Quantum Mechanics for Materials Engineers: The EMTO Method and Applications* (Springer Science & Business Media, 2007).

[52] S. O. Kart and T. Cagın, J. Alloys. Compds. **508**, 177 (2010).

[53] See Supplemental Material at http://link.aps.org/supplemental/10.1103/PhysRevB.96.174107 for detailed discussions on computational techniques related to calculations of elastic moduli and Curie temperatures, along with discussions on understanding atom projected magnetic moments from the electronic structures which include Refs. [56,57,74–77].

[54] H. Ebert, D. Koedderitzsch, and J. Minar, Rep. Prog. Phys. **74**, 096501 (2011).

[55] A. Liechtenstein, M. Katsnelson, V. Antropov, and V. Gubanov, J. Magn. Magn. Mater. **67**, 65 (1987).

[56] V. V. Sokolovskiy, V. D. Buchelnikov, M. A. Zagrebin, P. Entel, S. Sahoo, and M. Ogura, Phys. Rev. B **86**, 134418 (2012).

[57] D. Landau and K. Binder, in *A Guide to Monte Carlo Simulations in Statistical Physics* (Cambridge University Press, Cambridge, UK, 2000).

[58] S. Paul and S. Ghosh, J. Appl. Phys. **110**, 063523 (2011).

[59] V. Buchelnikov, V. Sokolovskiy, M. Zagrebin, M. Tufatullina, and P. Entel, J. Phys. D: Appl. Phys. **48**, 164005 (2015).

[60] V. V. Sokolovskiy, P. Entel, V. D. Buchelnikov, and M. E. Gruner, Phys. Rev. B **91**, 220409 (2015).

[61] G. D. Liu, X. F. Dai, H. Y. Liu, J. L. Chen, Y. X. Li, G. Xiao, and G. H. Wu, Phys. Rev. B **77**, 014424 (2008).

[62] H. Kandpal, G. Fecher, and C. Felser, J. Phys. D: Appl. Phys. **40**, 1507 (2007).

[63] Y. Feng, J. Y. Rhee, T. A. Wiener, D. W. Lynch, B. E. Hubbard, A. J. Sievers, D. L. Schlagel, T. A. Lograsso, and L. L. Miller, Phys. Rev. B **63**, 165109 (2001).

[64] T. Burch, T. Litrenta, and J. Budnick, Phys. Rev. Lett. **33**, 421 (1974).

[65] R. Helmholdt and H. Buschow, J. Less-Common Met. **128**, 167 (1987).

[66] S. Paul, B. Sanyal, and S. Ghosh, J. Phys.: Condens. Matter **25**, 236005 (2013).

[67] S. Paul, A. Kundu, B. Sanyal, and S. Ghosh, J. Appl. Phys. **116**, 133903 (2014).

[68] S. R. Barman, S. Banik, A. K. Shukla, C. Kamal, and A. Chakrabarti, Europhys. Lett. **80**, 57002 (2007).

[69] L. Wollmann, S. Chadov, J. Kübler, and C. Felser, Phys. Rev. B **90**, 214420 (2014).

[70] H. Luo *et al.*, J. Appl. Phys. **103**, 083908 (2008).

[71] A. Kundu and S. Ghosh, arXiv:1706.03425.

[72] H. Niu, X. Chen, P. Liu, W. Xing, X. Cheng, D. Li, and Y. Li, Sci. Rep. **2**, 718 (2012).

[73] S. Pugh, Philos. Mag. **45**, 823 (1954).

[74] A. Reuss, Z. Angew. Math. Mech. **9**, 49 (1929).

[75] T. Roy, M. Gruner, P. Entel, and A. Chakrabarti, J. Alloys. Compds. **632**, 822 (2015).

[76] T. Roy, D. Pandey, and A. Chakrabarti, Phys. Rev. B. **93**, 184102 (2016).
[77] W. Voigt, Ann. Phys. (NY) **274**, 573 (1889).
[78] D. Pettifor, Mater. Sci. Tech. **8**, 345 (1992).
[79] S. R. Barman and A. Chakrabarti, Phys. Rev. B **77**, 176401 (2008).
[80] K. Minakuchi, R. Umetsu, K. Kobayashi, M. Nagasako, and R. Kainuma, J. Alloys. Compd. **645**, 577 (2015).
[81] J. C. Slater, Phys. Rev. **49**, 537 (1936).
[82] L. Pauling, Phys. Rev. **54**, 899 (1938).
[83] D. Kikuchi, T. Kanomata, Y. Yamaguchi, H. Nishihara, K. Koyama, and K. Watanabe, J. Alloys. Compd. **383**, 184 (2004).